Nuclear Instruments and Methods in Physics Research B 269 (2011) 2297–2302

Contents lists available at ScienceDirect

Nuclear Instruments and Methods in Physics Research B

journal homepage: www.elsevier.com/locate/nimb

Micro-PIXE investigation of bean seeds to assist micronutrient biofortification

Cristina Cvitanich [a,*], Wojciech J. Przybyłowicz [b,1], Jolanta Mesjasz-Przybyłowicz [b], Matthew W. Blair [c], Carolina Astudillo [c], Elżbieta Orłowska [a], Anna M. Jurkiewicz [a], Erik Ø. Jensen [a], Jens Stougaard [a]

[a] Centre for Carbohydrate Recognition and Signalling, Department of Molecular Biology Aarhus University, Aarhus, Denmark
[b] Materials Research Department, iThemba LABS, P.O. Box 722, Somerset West 7129, South Africa
[c] CIAT – Centro International de Agricultura Tropical, Cali, Colombia

ARTICLE INFO

Article history:
Available online 1 March 2011

Keywords:
Micronutrient
Biofortification
Legume
Micro-PIXE
Seeds
Beans

ABSTRACT

This study compares the distribution and concentrations of micro- and macronutrients in different bean cultivars with the aim of optimizing the biofortification, a sustainable approach towards improving dietary quality. Micro-PIXE was used to reveal the distribution of Fe, Zn, Mn, Ca, P, S in seeds of common beans (*Phaseolus vulgaris*) and runner beans (*Phaseolus coccineus*). Average concentrations of elements in different tissues were obtained using ICP-AES. The highest concentrations of Zn in the studied beans were found in the embryonic axis, but an increased concentration of this element was also detected in the provascular bundles of the cotyledons. The first layer of cells surrounding provascular bundles accumulated high concentrations of Fe, while the next cell layer had an increased concentration of Mn. The analysis showed that the provascular bundles and the first cell layers surrounding them could have a significant role in the storage of important seed micronutrients – Zn, Fe, and Mn. This information has important implications for molecular biology studies aimed at seed biofortification.

1. Introduction

Micronutrient deficiencies affect a large proportion of the world population [1]. Fe deficiency is the most widespread nutritional disorder worldwide and has a negative impact on health, lifespan, and productivity. Zn deficiency results in increased risk of malaria, diarrhoea, pneumonia, and is estimated to be responsible for 4.4% of mortality of children less than 5 years old [2].

Micronutrient deficiencies affect primarily children and pregnant women in low-income, vulnerable populations, whose diets often rely on a few starchy staple crops. Biofortification by the breeding of staples with increased micronutrient content is a sustainable approach to reduce micronutrient malnutrition in these populations [3–7]. Legumes are micronutrient-rich, and, for example, Fe biofortification of common beans is expected to decrease the Fe deficiency burden by 9–33% in Northern Brazil [3,8,9].

Nutrient-rich seeds will not only be advantageous for combating malnutrition in humans, but can also improve food security by increasing seed vigor and thereby crop productivity. Low levels of micronutrients in seeds can negatively affect seed vigor and seedling vitality. Reduced vitality is primarily observed when nutrient-deficient seeds are grown in nutrient-poor soils [10,11]. For example, wheat plants grown on Zn-deficient siliceous sand produced more and bigger grains when they grew from seeds with higher Zn content compared to plants originating from seeds with less Zn [12]. Furthermore, a Zn-efficient genotype (a genotype that is able to absorb more Zn from Zn-deficient soils), had better fertilizer efficiency and a higher harvest index when grown under conditions of Zn deficiency in comparison with a Zn-inefficient genotype [12].

Two Zn-efficient genotypes of *Phaseolus vulgaris* accumulated 25% more Zn in their seeds compared to the two Zn-inefficient genotypes when Zn was present in the growth media [13]. While the two Zn-efficient genotypes did not have Zn deficiency symptoms, Zn-inefficient genotypes showed deficiency symptoms even when grown on soils with DTPA-extractable Zn values of 1.7 μg/g of soil. It has been suggested that high Zn content in seeds could be used for selecting Zn-efficient genotypes of *P. vulgaris*.

Information about the distribution of micronutrients within seed tissues can assist with the localization of sites of selective accumulation and barriers to the movement of micronutrients, in establishing how these elements are stored within the seed, and how they affect the nutritional status of the growing seedlings [11].

Knowledge of the distribution of micronutrients within mature seeds is limited. The distribution and concentration of Zn in wheat seeds was studied using diphenyl thiocarbazone staining [14]. It was found that Zn was concentrated in the embryo and aleurone parts of the seeds. In dicotyledons, synchrotron X-ray fluorescence

* Corresponding author. Tel.: +45 20 64 69 20; fax: +45 86 12 31 78.
E-mail address: crc@mb.au.dk (C. Cvitanich).
[1] On leave from the Faculty of Physics and Applied Computer Science, AGH University of Science and Technology, Kraków, Poland.

0168-583X/
doi:10.1016/j.nimb.2011.02.047

microtomography was used to study the elemental distribution in the model plant *Arabidopsis thaliana*. It was shown that Fe, Zn, and Mn accumulate in distinct regions within the mature seed cotyledon and radicle [15]. Furthermore, Fe distribution within the seed was affected by the disruption of the vacuolar Fe uptake transporter VIT1 [15,16]. In common beans, the distribution of micronutrients within the seeds of different genotypes was analyzed by measuring their concentration in dissected tissues [17–19]. In addition, micro-PIXE in combination with the Perls' Prussian blue staining method was used to study the accumulation and distribution of Fe in seeds of different common bean genotypes [20].

There are significant correlations between the concentrations of different nutrients in legume seeds [21–23]. For example strong correlations were found between the concentrations of Fe, Cu, Mg, Mn, and Zn in seeds from *Lotus japonicus* recombinant inbred lines [22]. In seeds from different *P. vulgaris* genotypes correlations were found between the concentrations of P, Fe, Zn, Cu and protein, and between Ca and Mn [23].

To reveal whether the correlation between the concentration of micro- and macronutrients is associated with their distribution within the seeds, micro-PIXE analysis has been used to determine the distribution of the nutritionally important elements Fe, Zn, Mn, Ca, P, and S within common bean and runner bean seeds.

2. Materials and methods

2.1. Plant material

P. vulgaris genotypes from both the Mesoamerican (small-seeded) and Andean (large-seeded) gene pools were obtained from the International Centre for Tropical Agriculture (CIAT), Cali, Colombia, and maintained either with the Genetic Resource Unit (G entries) or with the Bean Program (CAL, DOR and NUA lines) at CIAT. *Phaseolus coccineus* beans were purchased at a retailer in Denmark.

2.2. Average concentrations of elements in different tissues

For each genotype, 10–20 dry mature seeds were dissected into embryo axis, cotyledons, and seed coat tissues using a razor blade. Fe, Mn, and Zn content of each tissue was measured in duplicates at the Institute of Technology, Kongsvang Alle 29, 8000 Aarhus C, Denmark, using ICP-AES in the axial mode.

2.3. Micro-PIXE analysis

Dry bean seeds were cut with a razor blade and mounted on a thin Formvar layer. After coating the seed surfaces with carbon, microanalyses were performed using the nuclear microprobe at the Materials Research Department, iThemba LABS, South Africa. A proton beam of 3.0 MeV energy and 100–150 pA current was focused to a $3 \times 3\ \mu m^2$ spot and raster scanned over the areas of interest, using square or rectangular scan patterns with a variable number of pixels (up to 128×128). Micro-PIXE and proton backscattering spectrometry (BS) were used simultaneously as previously described [24–26]. Elemental concentrations and quantitative elemental images were obtained using GeoPIXE II software [27]. PIXE and BS spectra were extracted from selected regions of the analyzed tissue to obtain the average concentrations of the analyzed elements within them. The matrix composition and areal density were found from the analysis of BS spectra using RUMP simulation software [28]. The non-Rutherford cross-sections for a laboratory angle of 176° were calculated with SigmaCalc [29]. All specimens were thick and it was possible to use the same major element composition ($C_{34}H_{46}O_{16}K_{0.6}N_6$) in each case. Quantitative elemental images were generated using the *Dynamic Analysis* method using this matrix composition.

3. Results

3.1. The concentrations of Fe, Mn, and Zn in different bean tissues vary among genotypes

The concentrations of Fe, Mn, and Zn in the embryonic axis, cotyledons, and seed coats of *P. coccineus* and nine *P. vulgaris* genotypes were measured using ICP-AES (Table 1). The highest concentrations of Zn were found in the embryonic axis. In the measured samples, the embryonic axes contained between 53 and 80 μg/g of Zn. The concentrations of Zn in the cotyledons ranged between 17 and 30 μg/g and between 5 and 40 μg/g in the seed coats. Even though the embryonic axes contain the highest concentrations of Zn, this accounts for 2–5% of the total Zn content in the seeds. By far the largest amount of Zn can be found in the cotyledons, which represent 87–92% of the total seed weight. The cotyledons contain 83–94% of the total Zn in the studied seeds. Two *P. vulgaris* genotypes, G14519 and DOR364, contain relatively high percentage of their seed Fe in the seed coats. In these genotypes Fe in the seed coats accounts for 18% and 15% of the total seed Fe, respectively. For *P. coccineus* and the remaining *P. vulgaris* genotypes, the seed coats contain between 2% and 8% of the total seed Fe. Similar to Zn, the largest percentage of seed Fe was found in the cotyledons. This tissue contains 80–96% of the total seed Fe. Similar concentrations of Mn were measured in the cotyledons and embryonic axes, while lower Mn concentrations were detected in the seed coats. Variations in the concentrations of measured elements were observed among the studied beans. The analyzed beans from the *P.*

Table 1
Fe, Mn, and Zn concentrations in different tissues of mature *P. vulgaris* (*Pv.*) and *P. coccineus* seeds. Results obtained using ICP-AES in the axial mode. All values are averages of at least two measurements and are given in (μg/g). The relative standard deviations (% RSD) are below 16 for Fe, 10 for Mn and 9 for Zn. Part of Fe results was earlier reported in [20]. The detection limit for Fe, Mn, and Zn is 3 μg/g.

Genotype	Gene pool	Embryonic axis			Cotyledon			Seed coats		
		Fe	Mn	Zn	Fe	Mn	Zn	Fe	Mn	Zn
Pv. G14519	M	70	13	72	65	14	29	132	4.4	14
Pv. G4825	M	67	14	68	56	14	24	56	3.9	5
Pv. DOR364	M	46	14	75	43	20	34	71	3.8	11
Pv. CAL96	A	81	12	65	57	18	27	17	3.2	32
Pv. NUA35	N/A	103	14	64	80	23	30	61	4.5	16
Pv. NUA45	N/A	84	11	65	47	16	18	26	3.7	20
Pv. G19833	A	85	13	71	58	14	27	30	4.4	40
Pv. G21242	A	97	16	80	70	15	28	42	5.0	28
Pv. G21078	A	53	12	53	43	15	19	23	4.2	6
P. coccineus	N/A	84	20	79	45	17	17	35	6.6	22

vulgaris genotype NUA35 showed the highest average Fe and Mn concentrations, and had the second highest concentration of Zn in the cotyledons. In comparison to its parental lines (CAL96 and G14519) the cotyledons of NUA35 contained higher concentrations of these three elements.

3.2. In the cotyledons of P. coccineus and P. vulgaris seeds, micronutrients accumulate in distinctive patterns

Micro-PIXE analyses were used to reveal how nutrients are distributed within mature bean seeds (Fig. 1). The present study fo-

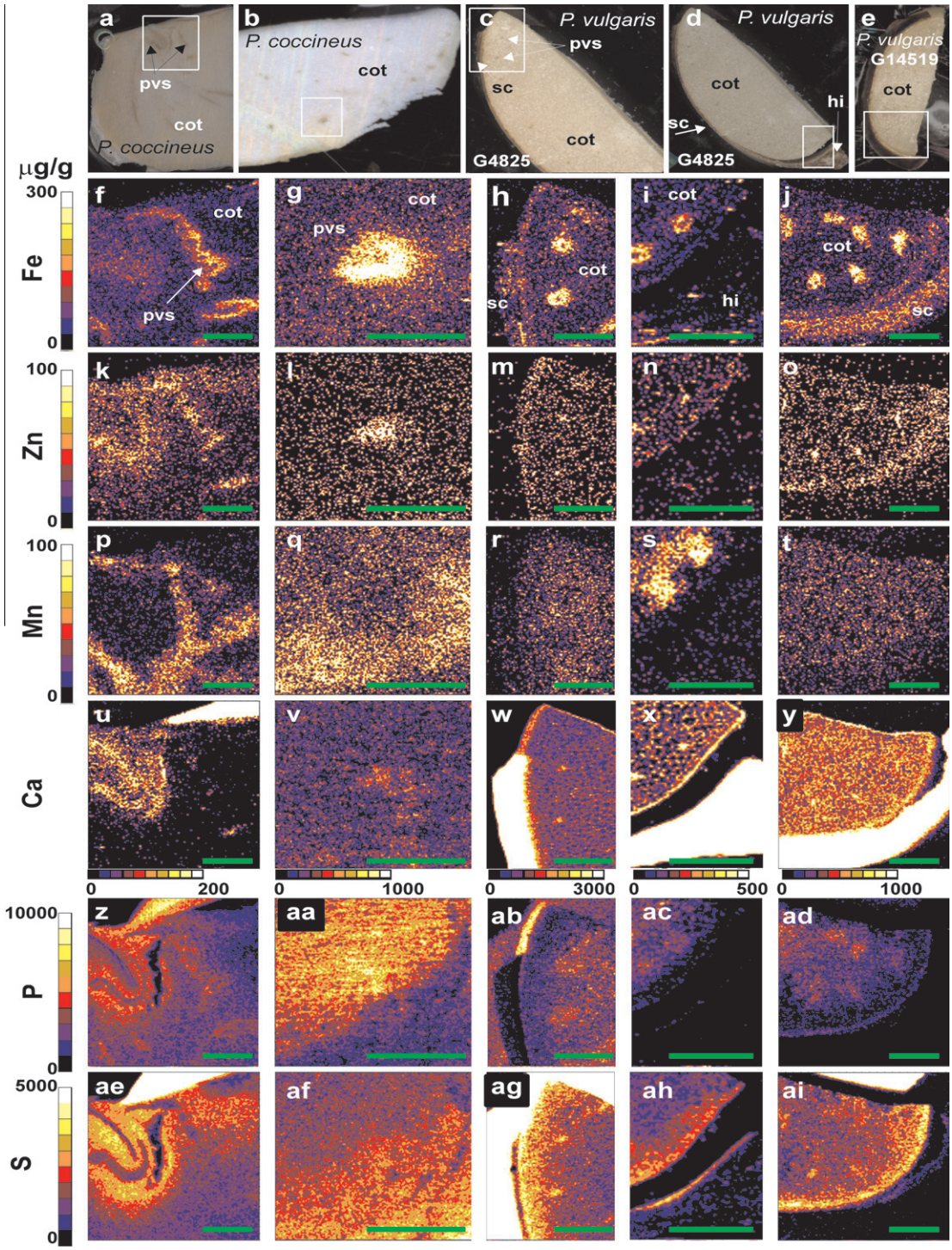

Fig. 1. Elemental analysis of common beans and runner beans using micro-PIXE. a–e: optical micrographs of the analyzed seed tissue. The scanned areas are indicated by an open square. a, b: *P. coccineus*, c, d: *P. vulgaris* G4825, e: *P. vulgaris* G14519. Maps of Fe (f–j), Zn (k–o), Mn (p–t), Ca (u–y), P (z–ad), and S (ae–ai) are shown. The elemental maps shown in the first (f, k, p, u, z and ae), second (g, l, q, v, aa and af), third (h, m, r, w, ab, and ag), fourth (I, n, s, x, ac, and ah), and fifth (j, o, t, y, ad, and ai) columns correspond to the areas indicated in a, b, c, d, and e, respectively. The concentration scales are shown on the left side, all the values are given in µg/g dry weight. For Ca the concentration scales are shown underneath the respective maps. The scale bars are 0.5 mm. Abbreviations: cot: cotyledon, hi: hilum, pvs: provascular tissue, sc: seed coat. b, d, e, j, and ad have been previously published [20].

cused on the cotyledons as these parts of seeds contain the highest amounts of Fe, Mn, and Zn. As previously reported [20], Fe accumulates in the cotyledon cells that surround the provascular bundles and in the seed coats of the *P. vulgaris* genotype G14519 (Fig. 1f–j).

In the cotyledons of mature seeds Zn is more evenly distributed; however higher concentrations of this element accumulate near the provascular bundles (Fig. 1k–o). For example the regions 7, 15, 25, and 32 (color lilac in Fig. 2) have average Zn concentrations between 61 and 165 μg/g, at least twice as high as average Zn values in the cotyledons measured by ICP-AES (17–29 μg/g, Table 1). In addition, the lilac regions contain between 10% and 150% higher concentrations of Zn than the red regions.

Interestingly, the concentrations of Mn were lower in the Fe-rich regions compared to the surrounding tissue (Fig. 1p–t). For example the regions 8 + 9, 13, 19 + 20, 24, and 29 + 30 + 31 (red in Fig. 2) contained 80, 80, 50, 70, and 40% less Mn than the proximal regions 6, 12, 18, 21, and 28 (Fig. 2, Table 2). The concentration of Mn in the Fe-rich regions is similar to the average

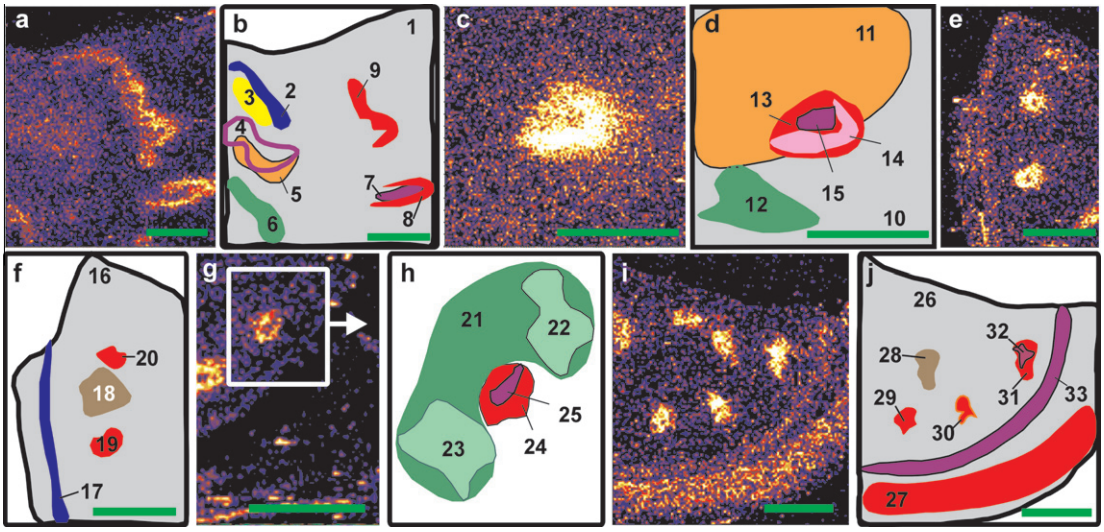

Fig. 2. Regions selected for elemental quantifications. a, c, e, g, and i: Fe maps of the tissue. The regions are color coded based on the elements used for their selection: grey – background; red – Fe; lilac – Zn; green – Mn; blue – Ca; orange – P; yellow – S. Each region is annotated with a unique number shown in Table 2. The open box in g illustrates the area of the tissue used for the selection of regions. The scale bars are 0.5 mm. (For interpretation of the references to color in this figure legend, the reader is referred to the web version of this paper.)

Table 2
Concentrations of micro- and macronutrients in different regions of *P. coccineus* and *P. vulgaris* cotyledons. Average (Avg) concentrations of elements in selected regions shown in the maps of Fig. 2b, d, f, h, and j. Colors correspond to the colors of regions in Fig. 2. The uncertainties (+/−) are given in the right side of each column. All values are reported in μg/g.

Region	Fe		Zn		Mn		Ca		P		S	
	Avg	+/−	Avg	+/−	Avg	+/−	Avg	+/−	Avg	+/−	Avg	+/−
1	69	5	27	2	31	2	341	11	3260	88	2350	38
2	77	3	31	2	11	2	344	21	3500	145	2500	172
3	81	3	31	4	8	2	297	17	4130	184	3820	265
4	87	3	69	3	7	1	287	22	4700	206	2320	197
5	70	3	46	2	6	1	247	20	5090	252	3270	256
6	53	2	19	2	93	3	105	13	3330	206	1960	181
7	136	5	71	5	<4.	2	195	24	3840	191	1440	170
8 + 9	189	5	43	2	17	1	114	10	3840	154	1720	131
10	80	9	21	2	36	4	183	22	4130	107	1850	83
11	100	16	21	4	23	5	137	35	5390	229	1390	107
12	69	9	23	3	81	12	127	19	2780	197	2160	172
13	350	19	65	4	19	3	255	18	5750	175	1900	112
14	476	24	54	7	19	4	235	23	5590	178	1990	112
15	320	23	165	15	17	4	361	28	6470	203	2010	109
16	67	5	19	2	13	1	2030	48	2120	90	3030	52
17	88	7	12	4	<4.	2	21320	77	295	43	3710	58
18	55	5	24	5	35	3	480	27	2330	91	1800	58
19 + 20	414	14	46	6	16	4	643	28	3840	117	2300	66
21	52	2	16	1	93	4	239	28	2540	195	1260	168
22 + 23	45	3	19	2	123	5	257	22	2270	130	1470	123
24	187	9	35	7	24	5	398	28	3410	204	1730	226
25	185	21	61	17	23	8	545	41	3520	277	1990	135
26	71	4	28	1	8	1	1170	28	1170	57	1240	32
27	124	5	13	2	2	1	3860	40	33	13	220	7
28	49	5	25	6	22	4	194	18	1963	90	1344	46
29 + 30 + 31	273	8	84	8	14	2	268	15	2129	89	1896	60
32	411	22	96	28	15	6	353	30	2388	185	2184	124
33	60	3	43	3	13	2	296	17	1078	63	2870	60

concentration of Mn in the cotyledons that is 17 μg/g for *P. coccineus* and 14 μg/g for *P. vulgaris* G4825 and G14519 (Table 1). The highest Mn concentration was found in the regions 22 and 23, proximal to the Fe-rich region in *P. vulgaris* G4825 (Fig. 2 and Table 2). The average Mn concentration in these regions is 123 μg/g, almost nine times higher than the average concentration in the cotyledons.

3.3. The macronutrients P, S, and Ca also show unique patterns of accumulation

With the exception of the provascular regions, P and S show inverse gradients of concentrations (Fig. 1aa–ad compared to af–ai). While the concentrations of S increase towards the epidermis, the concentrations of P decrease when approaching this layer. For example, region 10 contains higher S and lower P concentrations than region 11 (Fig. 2, Table 2). A slight increase in the concentrations of these two elements can be observed in the provascular regions as illustrated by region 5 that contains 5090 μg/g of P and 3270 μg/g of S. These concentrations are respectively 56% and 39% higher than the respective concentrations in the analyzed tissue (Fig. 2, region 1).

Similar to Zn, a slight increase in the concentration of Ca was observed in the provascular bundles (Fig. 1u–y). The concentration of Ca in the regions shown in lilac (Fig. 2 and Table 2, regions 7, 15, 25, and 32) is 30–60% higher than in the larger regions shown in red (Fig. 2 and Table 2, regions 8, 13, 24, and 31, respectively). Comparison of the concentrations of Fe, Zn, and Ca in the regions 14 and 15 (Fig. 2 and Table 2) shows that region 14 has the highest Fe concentration (476 μg/g), while the proximal region 15 has lower Fe concentration (320 μg/g) but higher Zn (165 compared to 54 μg/g) and Ca concentrations (361 compared to 235 μg/g).

Apart from slightly increased Ca concentration near the provascular tissue, the highest Ca concentrations were found in the seed coats (Fig. 1u–y). This tissue contains more than 3000 μg/g of Ca. For example in region 27, which outlines the Fe-rich part of the seed coat in the *P. vulgaris* genotype G14519, Ca concentration is 3860 μg/g, while much higher concentrations of this element (21,320 μg/g) were measured in region 17. This is the region of the highest Ca concentration (Figs. 1 and 2, Table 2). Ca concentrations in the seed coats are more than 10 fold higher than in any other marked regions outside seed coat tissues.

4. Discussion

Different studies have shown that there is a positive correlation between the concentrations of Fe and Zn in the *Phaseolus* seeds [8,21,23,30]. Our study shows that the embryonic axes are rich in Fe and Zn and that both elements are accumulated at elevated concentrations in the provascular region. The highest concentrations of Zn in seeds of *P. coccineus* and *P. vulgaris* were detected in the embryonic axis, but a slightly increased concentration of Zn was also measured in the provascular bundles of the cotyledons. Fe, Zn, and Mn are accumulated in almost exclusive patterns in the proximity of each other. Here Zn is surrounded by Fe, which in turn is surrounded by Mn. In comparison, analysis of the cotyledons of soybean seeds did not show any unique accumulation pattern of these elements [31]. The distribution patterns of Fe, Zn and Mn in the studied *Phaseolus* seeds are more similar to that in the *A. thaliana* seeds than in the soybeans. Synchrotron X-ray fluorescence microtomography analysis of *A. thaliana* seeds showed an elevated concentration of Zn in the provascular tissue of the radicle and cotyledons [15]. The presence of higher concentration of Zn in the provascular cells indicates that this element could be easily mobilized to the growing parts of the seedling during germination.

In the studied *Phaseolus* seeds, 2–18% of the seed Fe was found in the seed coats [20] which comprise 7–10% of seed dry weight, while in soybean 20–40% of the seed Fe was found in the seed coat, which comprises 6–8% of the total soybean seed dry weight [31]. It is interesting that although they are legumes, the highest concentrations of Fe in soybeans were found in the seed coats and in the provascular cells of the radicle [31], while in the studied *Phaseolus* species the highest Fe concentrations were found in the cells surrounding the provascular tissue of the cotyledons [20]. This indicates that the transporters involved in the mobilization of Fe to the embryo could be active at different time points of seed and seedling development in these species. As was shown for *Phaseolus* seeds, in *A. thaliana* Fe accumulates in cells surrounding the provascular bundles of both the cotyledons and radicles [15,16].

Elevated Mn concentrations accumulated in the tissue surrounding the Fe-rich regions in the *Phaseolus* cotyledons. It is remarkable that in the soybean embryonic axis Mn is accumulated in a pattern similar to Fe, with the exception of the observed accumulation of Mn in the procambium cells of the radicle, where Fe concentration was relatively low [31]. Again, regarding the distribution of this element, the *Phaseolus* seeds are more similar to *A. thaliana* than to soybean seeds. In *A. thaliana* Mn was detected in the cotyledonary tissue surrounding the Fe-rich regions [15].

Energy dispersive X-ray analysis of globoid crystals from dry tomato (*Lycopersicon esculentum*) seeds revealed that these crystals always contained P, K, and Mg, and that some globoid crystals also contained small amounts of Ca, Mn, and Fe [32]. Globoid crystals in protodermal cells of tomato seeds often contained Mn and Fe, while in the provascular tissue they often contained Fe, and in cells that surround the provascular tissues they always contained Fe [32]. These results are in agreement with the specific distribution of Mn and Fe within seed tissues and confirm the accumulation of these micronutrients in or near the provascular tissues. They also indicate that Fe and Mn in these tissues might be present in the phytin aggregates [32].

Interestingly, a strong positive correlation has been found between Ca and Mn concentration in *P. vulgaris* seeds [23]. Our studies indicate that the Ca concentrations tend to be lower where Mn concentrations are the highest. In addition Mn concentrations tend to be low in the seed coat, the epidermal cell layers, and in the provascular bundles where Ca concentrations are higher. Further studies are needed to reveal the biological mechanisms behind the differential patterns of accumulation of elements and the impact of these mechanisms on elemental concentrations in the seeds.

Zn and Ca accumulate in a similar pattern within the cotyledons of the analyzed *Phaseolus* species, but the highest concentrations of Ca were found in the seed coats of all the studied legumes. These results are in agreement with the results for castor beans, *Ricinus communis* [33]. It has been suggested that Ca in the seed coat of castor beans was present as crystals of Ca oxalate, not likely available for the seedlings during germination. In a different study it was shown that less than 30% of the cotyledonary Ca in pea seeds was mobilized to the growing seedlings [34]. The accumulation of a slightly higher concentration of Ca in the provascular bundles of the *Phaseolus* cotyledons leads to the speculation that this Ca could be more available to the growing seedlings than the Ca present in the seed coat and in the surrounding cotyledonary tissue.

Our results show that the distribution of micro- and macronutrients in seeds is species- dependent. This is in agreement with previous reports. For example, the distribution patterns of Ca were different in castor beans compared to the patterns in seeds of *Cucurbita* species [33]. Differences in the accumulation of micronutrients among seed tissues indicate that different mechanisms might regulate the nutrient transport to target sites within the seeds. For example, it is possible that a common metal transporter is responsible for the accumulation of both Fe and Mn in the pro-

vascular bundles of the soybean radicle, but that cell-specific transporters are involved in the differential accumulation of Fe, Zn, and Mn in the cotyledons of *P. coccineus*.

5. Conclusions

This study revealed the accumulation sites of micro- and macronutrients in two important crop legumes, common beans and runner beans. This information is crucial for future studies of the molecular mechanisms responsible for the micronutrients' accumulation in legume seeds. Furthermore, it will help in understanding of how dietary nutrients stored in seeds can affect the developing plant. Major differences in the accumulation patterns of nutrients have been found, even between closely related species. These findings suggest that there might be limitations in the applicability of exploiting genes discovered in the model plants to improve the nutritional value of other species.

In addition, this work provides fundamental information that will assist the development of biofortified crops and the study of micronutrient bioavailability.

Acknowledgments

Funding was provided by the Centre for Carbohydrate Recognition and Signalling; the Danish Agency for Science, Technology and Innovation; HarvestPlus; International Atomic Energy Agency, and the Research Foundation of the University of Aarhus, Denmark. The authors are grateful for the technical assistance of Finn Pedersen, Kirsten Sørensen, and Hanne Busk.

References

[1] WHO (World Health Organization). Micronutrient deficiencies. Iron deficiency anaemia. http://www.wpro.who.int/health_topics/micronutrient_deficiencies. http://www.who.int/nutrition/topics/ida/en/index.html. Accessed 27 Oct 2009.
[2] R.E. Black, L.H. Allen, Z.A. Bhutta, L.E. Caulfield, M. de Onis, M. Ezzati, C. Mathers, J. Rivera, Lancet 371 (2008) 243.
[3] J.V. Meenakshi, N. Johnson, V.M. Manyong, H. De Groote, J. Javelosa, D. Yanggen, F. Naher, C. Gonzalez, J. Garcia, E. Meng, How cost-effective is biofortification in combating micronutrient malnutrition? An ex-ante assessment. http://www.harvestplus.org, in 2007.
[4] P. Nestel, H.E. Bouis, J.V. Meenakshi, W. Pfeiffer, J. Nutr. 136 (2006) 1064.
[5] A.J. Stein, J.V. Meenakshi, M. Qaim, P. Nestel, H.P. Sachdev, Z.A. Bhutta, Soc. Sci. Med. 66 (2008) 1797.
[6] R.M. Welch, R.D. Graham, J. Exp. Bot. 55 (2004) 353.
[7] R.M. Welch, R.D. Graham, Plant Soil 245 (2002) 205.
[8] R.M. Welch, W.A. House, S. Beebe, Z. Cheng, J. Agr. Food Chem. 48 (2000) 3576.
[9] W.J. Broughton, G.H. Hernandez, M. Blair, S. Beebe, P. Gepts, J. Vanderleyden, Plant Soil 252 (2003) 55.
[10] R.M. Welch, in: Z. Rengel (Ed.), Mineral Nutrition of Crops: Fundamental Mechanisms and Implications, Food Products Press, 2000, p. 206.
[11] R.M. Welch, Adv. Plant Nutr. 2 (1986) 205.
[12] Z. Rengel, R.D. Graham, Plant Soil 173 (1995) 267.
[13] J.T. Moraghan, K. Grafton, Soil Sci. Soc. Am. J 63 (1999) 918.
[14] L. Ozturk, M.A. Yazici, C. Yucel, A. Torun, C. Cekic, A. Bagci, H. Ozkan, H.-J. Braun, Z. Sayers, I. Cakmak, Physiol. Plant 128 (2006) 144.
[15] S.A. Kim, T. Punshon, A. Lanzirotti, L. Li, J.M. Alonso, J.R. Ecker, J. Kaplan, M.L. Guerinot, Science 314 (2006) 1295.
[16] H. Roschzttardtz, G. Conejero, C. Curie, S. Mari, Plant Physiol. (2009), doi:10.1104/pp.1109.144444.
[17] L.O. Tiffin, R.L. Chaney, Plant Physiol. 52 (1973) 393.
[18] J.A. Laszlo, J. Plant Nutr. 13 (1990) 231.
[19] M. Ariza-Nieto, M.W. Blair, R.M. Welch, R.P. Glahn, J. Agr. Food Chem. 55 (2007) 7950.
[20] C. Cvitanich, W.J. Przybyłowicz, D.F. Urbanski, A.M. Jurkiewicz, J. Mesjasz-Przybyłowicz, M.W. Blair, C. Astudillo, E.Ø. Jensen, J. Stougaard, BMC Plant Biol. 10 (2010) 26.
[21] G.M. Tryphone, S. Nchimbi-Msolla, Afr. J. Agric. Res. 5 (2010) 738.
[22] M.A. Klein, M.A. Grusak, Genome 52 (2009) 677.
[23] C. Pinheiro, J.P. Baeta, A.M. Pereira, H. Domingues, C.n.P. Ricardo, J. Food Compos. Anal. 23 (2010) 319.
[24] V.M. Prozesky, W.J. Przybyłowicz, E. Van Achterbergh, C.L. Churms, C.A. Pineda, K.A. Springhorn, J.V. Pilcher, C.G. Ryan, J. Kritzinger, H. Schmitt, T. Swart, Nucl. Instrum. Meth. Phys. Res. B 104 (1995) 36.
[25] W.J. Przybyłowicz, J. Mesjasz-Przybyłowicz, P. Migula, M. Nakonieczny, M. Augustyniak, M. Tarnawska, K. Turnau, P. Ryszka, E. Orłowska, S. Zubek, E. Głowacka, X Ray Spectrom. 34 (2005) 285.
[26] W.J. Przybyłowicz, J. Mesjasz-Przybyłowicz, C.A. Pineda, C.L. Churms, K.A. Springhorn, V.M. Prozesky, X Ray Spectrom. 28 (1999) 237.
[27] C. Ryan, Int. J. Imag. Syst. Tech. 11 (2000) 219.
[28] L.R. Doolittle, Nucl. Instrum. Methods B 15 (1996) 227.
[29] http://www-nds.iaea.org/sigmacalc/. Accessed 30 May 2010.
[30] M. Blair, C. Astudillo, M. Grusak, R. Graham, S. Beebe, Mol. Breeding 23 (2009) 197.
[31] C. Cvitanich, W.J. Przybylowicz, J. Mesjasz- Przybylowicz, M.W. Blair, E.O. Jensen, J. Stougaard, Iron, zinc, and manganese distribution in mature soybean seeds, in: eScholarship Repository, Proc. Int. Plant Nutr. Coll. XVI. http://escholarship.org/uc/item/6mh1d8vv, 2009.
[32] E. Spitzer, J.N.A. Lott, Can. J. Bot. 58 (1980) 699.
[33] .N.A. Lott, J.S. Greenwood, C.M. Vollmer, Plant Physiol. 69 (1982) 829.
[34] I.B. Ferguson, E.G. Bollard, Ann. Bot. 40 (1976) 1047.